

**Supplementary Material to the Paper:  
Conservative Scale Recomposition for Multiscale Denoising  
(The Devil is in the High Frequency Detail)**

Gabriele Facciolo\*, Nicola Pierazzo\*, and Jean-Michel Morel\*

---

**Abstract.** This document contains supplementary figures not shown in the main article.

**Detailed SSIM index for training.** In Figure 1 we report the average SSIM changes over the training database. Note that overall SSIM and PSNR (in the main document) have a similar behaviors.

**Detailed analysis of test results.** Figure 3 shows the detailed PSNR gains due to the multiscale algorithm for all the images in the test set. For most methods the average gain is monotonic with the noise level, with the exception of NL-Bayes. This is can be explained because NL-Bayes uses different parameter sets (including patch and neighborhood sizes) depending on the noise level. Improving this behavior would require to adapt the multi-scale parameters to each level of the pyramid for each level of noise. We also note that for all the test images the gain is strictly positive in terms of SSIM, and mostly positive in PSNR (except for some small fluctuations).

**All the Crops.** Figures 4-7 show the results of both DCT and Laplacian pyramids.

**REFERENCES**

- [1] H. C. BURGER AND S. HARMELING, *Improving denoising algorithms via a multi-scale meta-procedure*, in Lecture Notes in Computer Science (including subseries Lecture Notes in Artificial Intelligence and Lecture Notes in Bioinformatics), vol. 6835 LNCS, 2011, pp. 206–215, [doi:10.1007/978-3-642-23123-0\\_21](https://doi.org/10.1007/978-3-642-23123-0_21).

---

\*CMLA, ENS Paris Saclay, Cachan, France.

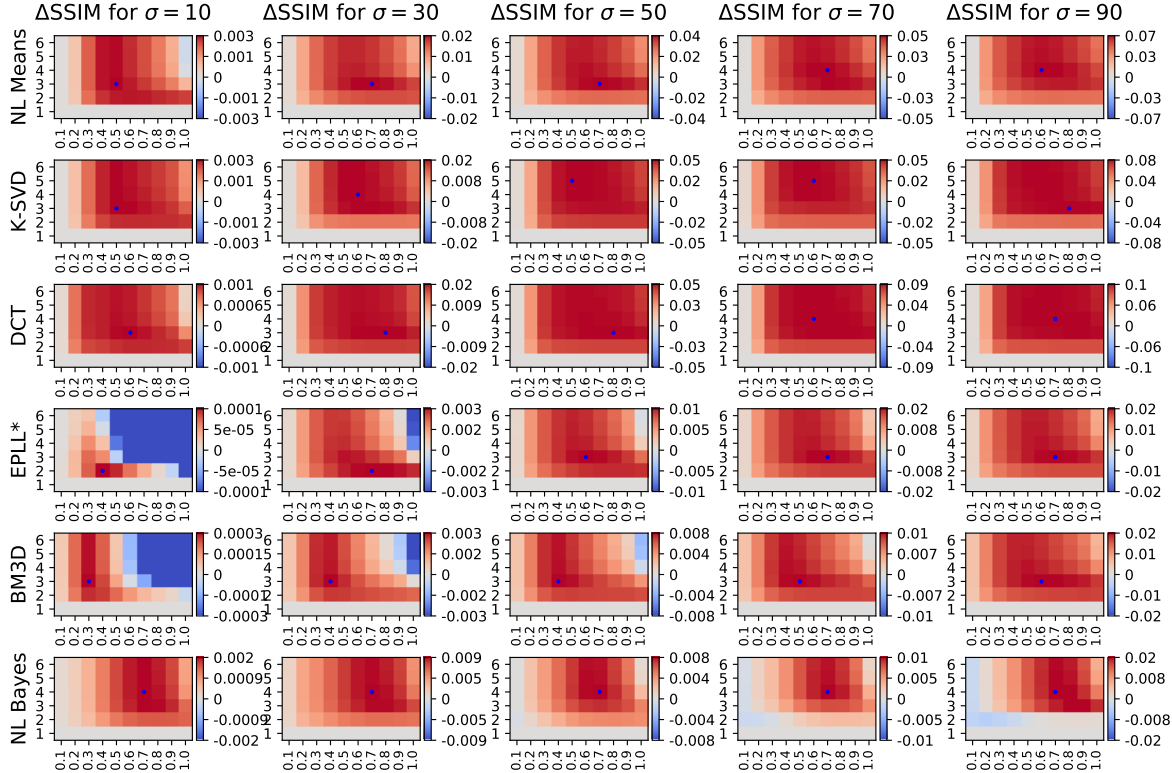


Figure 1: Average SSIM changes obtained with different parameters of the DCT Multi-Scale Framework applied to different denoising algorithms for different noise levels. The integers on the left of each figure (1, 2, ..., 6) represent the number of scales  $n_{scales}$  used in Algorithm. The bottom row of each graphic corresponds to the single-scale algorithm for which  $\Delta\text{SSIM} = 0$ . The value at the bottom is the fraction  $f_{rec}$  of low frequencies at each scale being used in the recomposition.

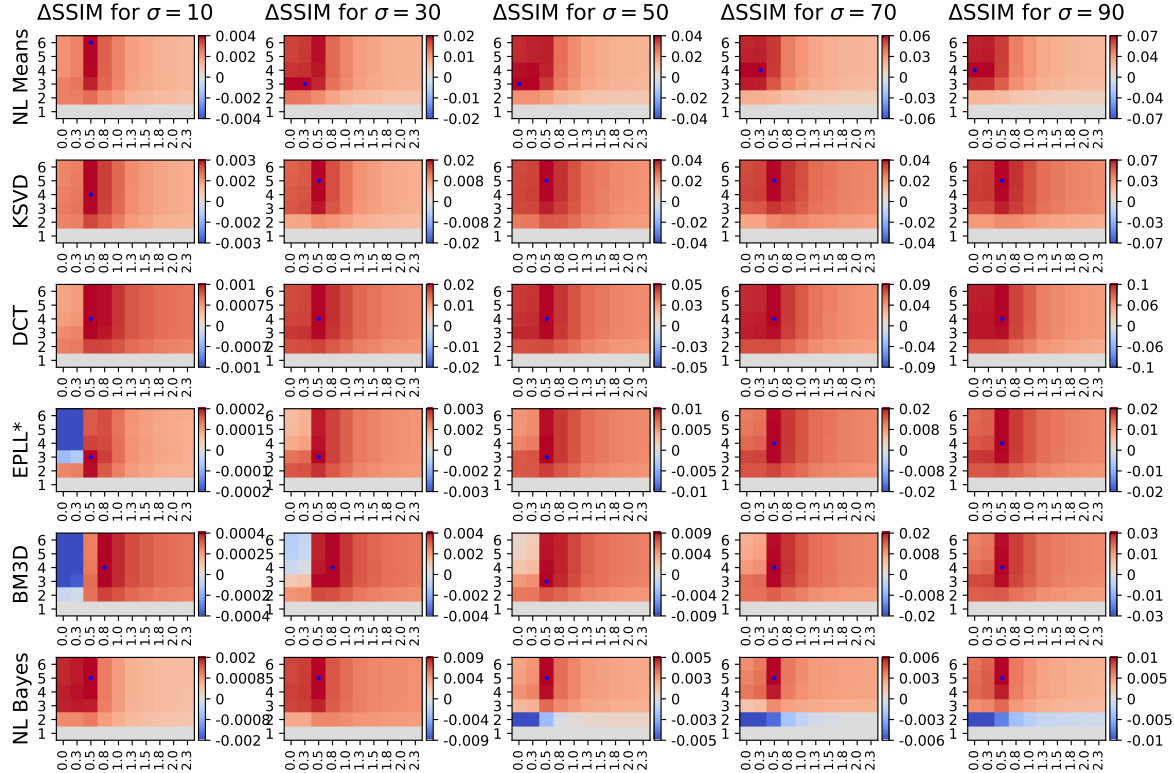


Figure 2: Average SSIM changes obtained with different parameters of the Laplacian Multi-Scale Framework applied to different denoising algorithms for different noise levels. The integers on the left of each figure (1, 2, ..., 6) represent the number of scales  $n_{\text{scales}}$  used in Algorithm. The bottom row of each graphic corresponds to the single-scale algorithm for which  $\Delta\text{SSIM} = 0$ . The value at the bottom is the standard deviation  $\gamma$  of the low-pass filtering Gaussian used in the conservative recomposition.

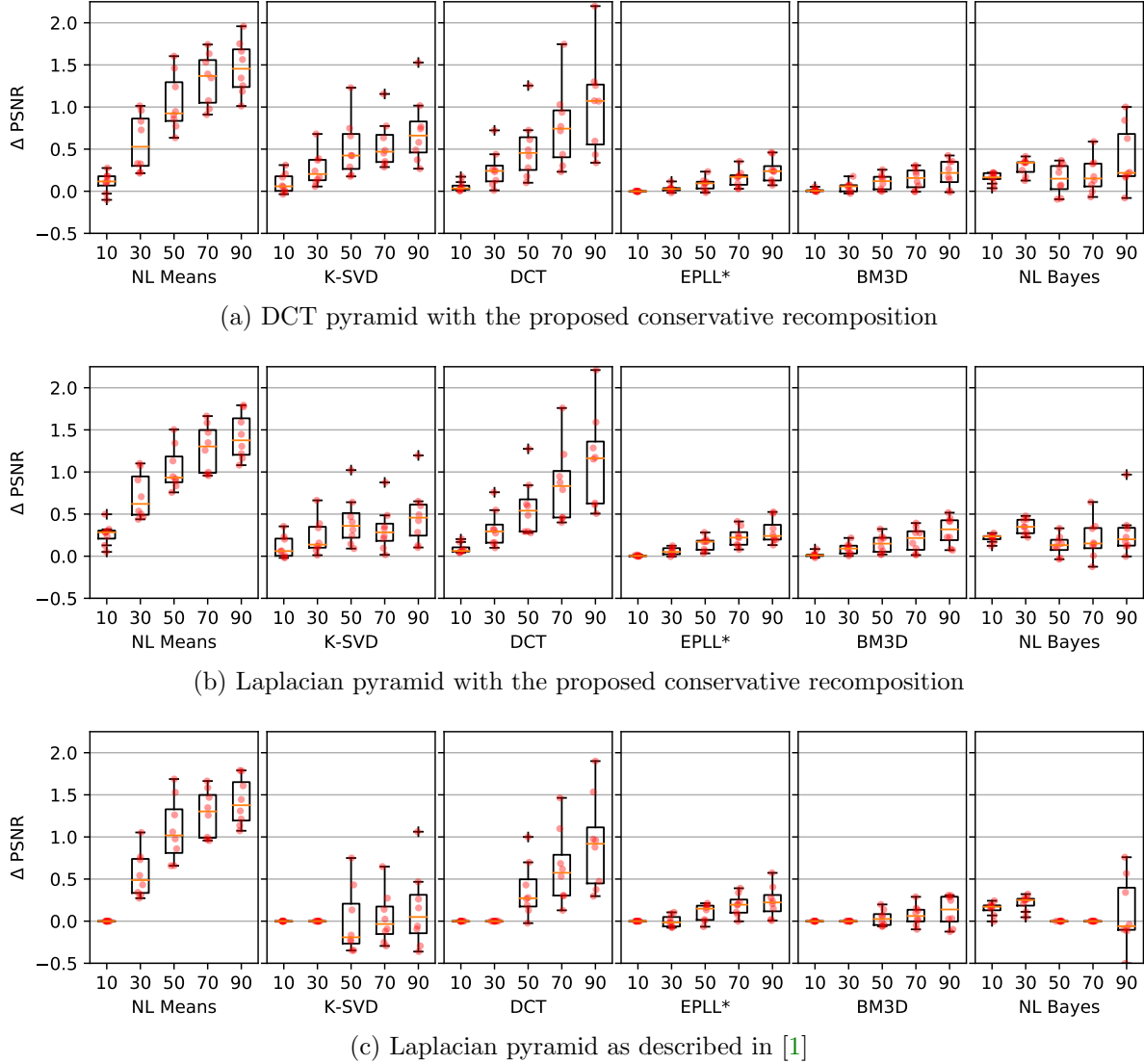


Figure 3: PSNR gain (in dB) obtained on the test image dataset applying the Multi-Scale Framework with the DCT and Laplacian pyramids with respect to the single-scale version of different denoising algorithms. Each algorithm and noise level with the corresponding optimal parameters computed on the training images. This illustrates two facts: a) that the PSNR gain is systematic; only a few images show a very slight PSNR loss; b) the conservative recomposition is also systematically better. Even if the PSNR gain is moderate, the visual gain is nevertheless apparent.

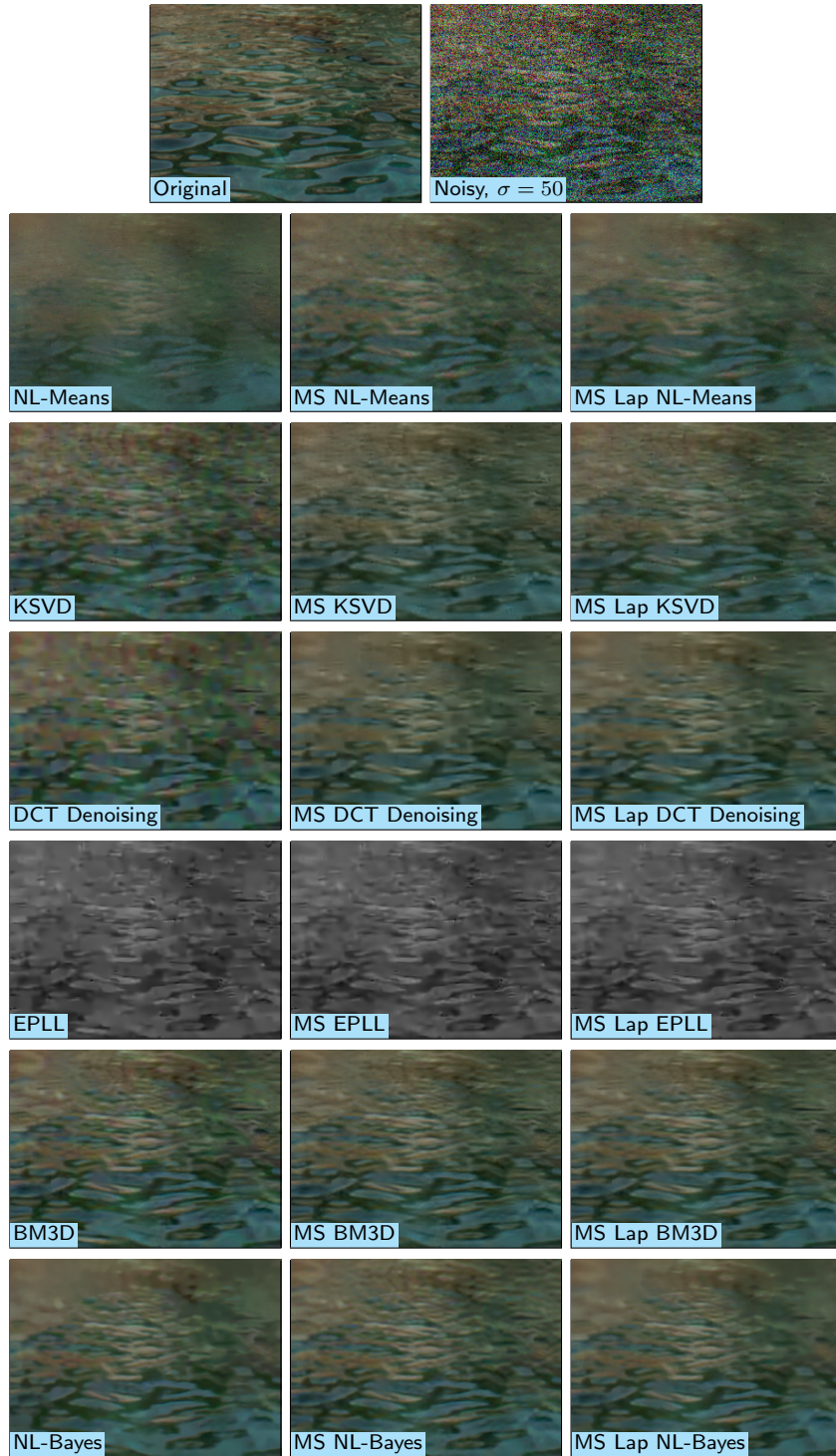


Figure 4: Results of the Single-Scale and Multi-Scale (with DCT and Laplacian pyramids) algorithms. The details are taken from the set of test images. For all algorithms, one can observe a removal of spurious oscillation in smooth regions (water, glass) and a gain in detail sharpness.

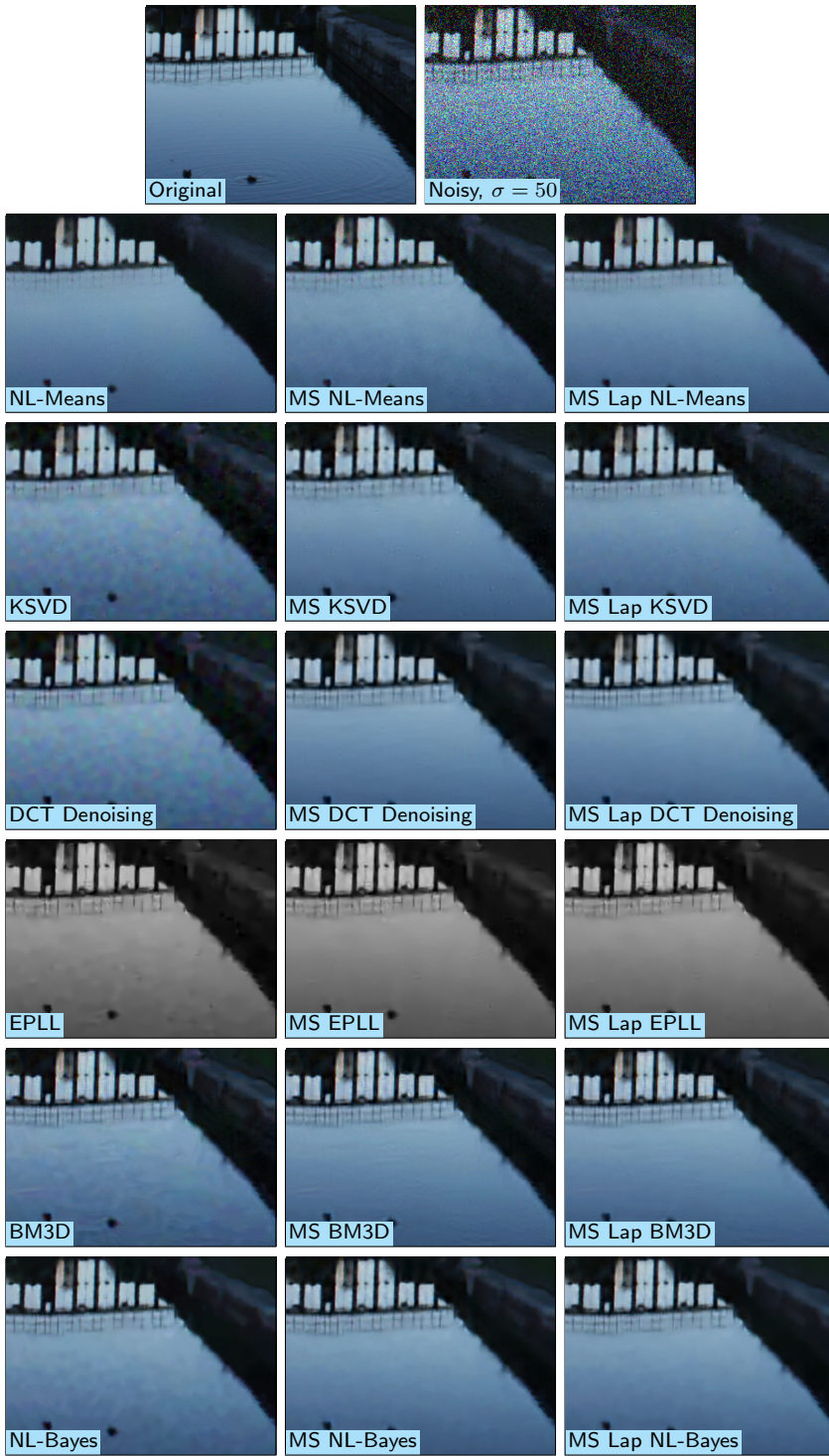


Figure 5: Results of the Single-Scale and Multi-Scale (with DCT and Laplacian pyramids) algorithms. The details are taken from the set of test images. For all algorithms, one can observe a removal of spurious oscillation in smooth regions (water, glass) and a gain in detail sharpness.

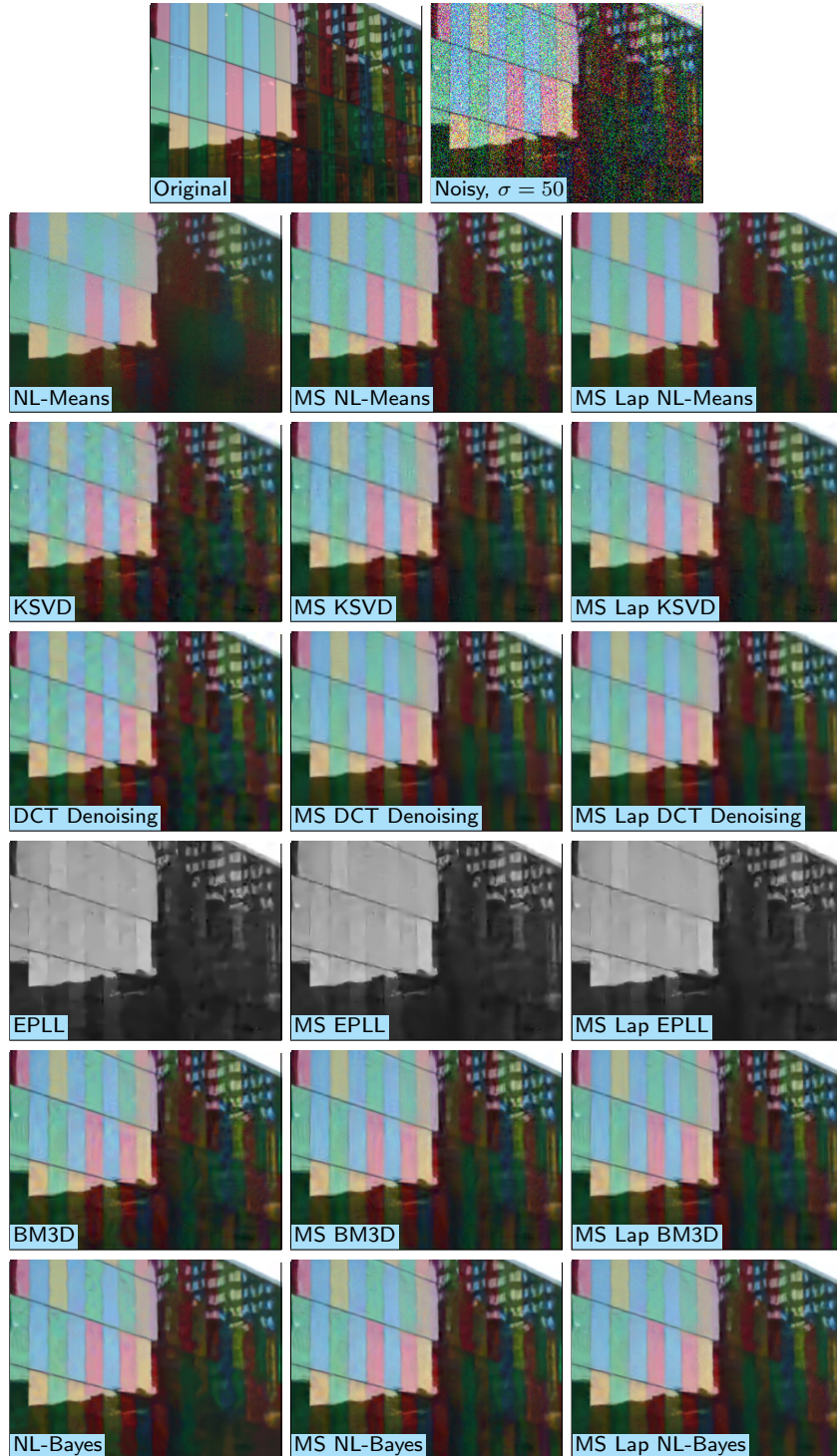


Figure 6: Results of the Single-Scale and Multi-Scale (with DCT and Laplacian pyramids) algorithms. The details are taken from the set of test images. For all algorithms, one can observe a removal of spurious oscillation in smooth regions (water, glass) and a gain in detail sharpness.

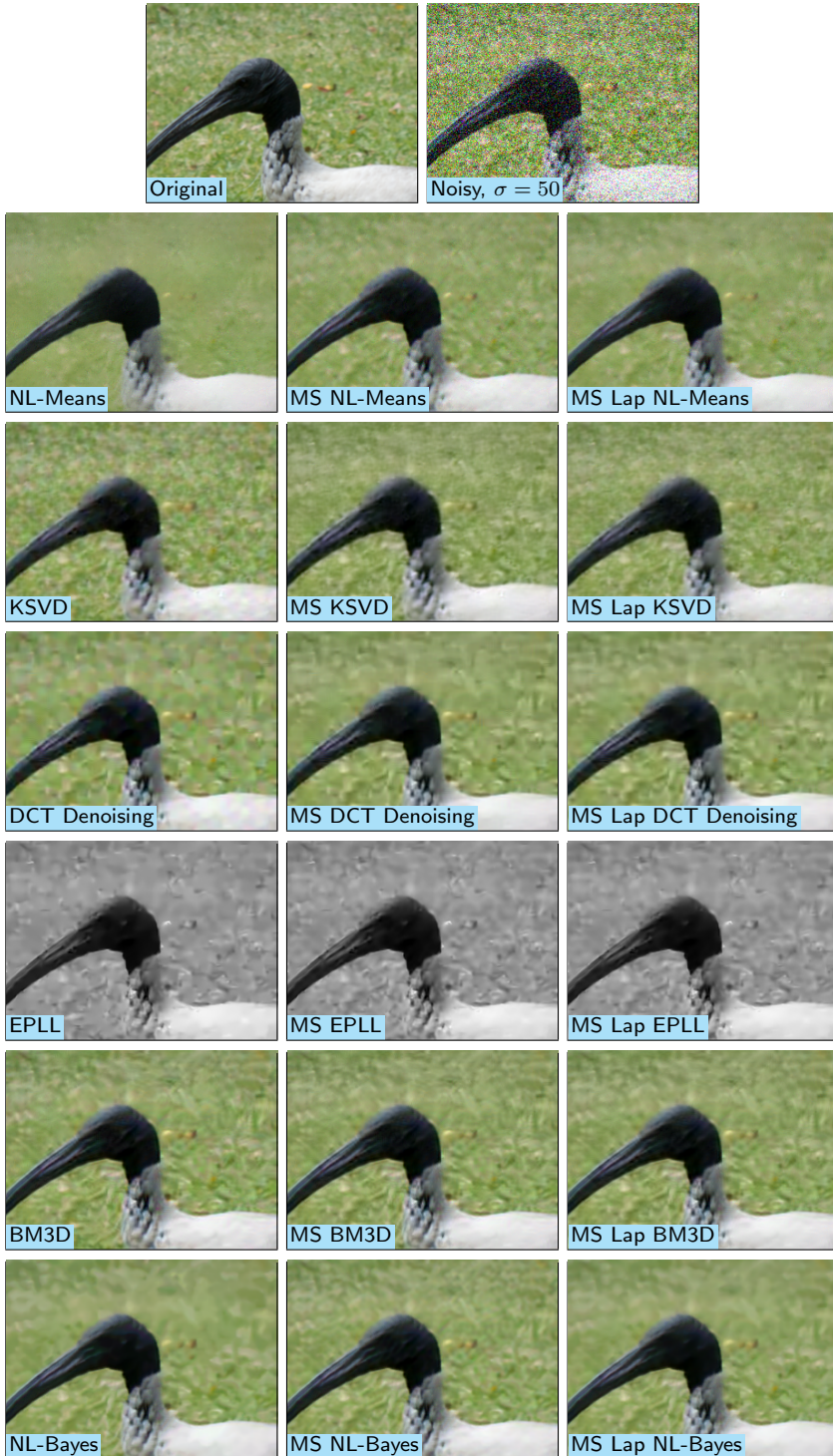


Figure 7: Results of the Single-Scale and Multi-Scale (with DCT and Laplacian pyramids) algorithms. The details are taken from the set of test images. For all algorithms, one can observe a removal of spurious oscillation in smooth regions (water, glass) and a gain in detail sharpness.